

Classical Preheating and Decoherence

D. T. Son

Department of Physics FM-15, University of Washington

Seattle, WA 98105, USA

January 1996

Abstract

We establish the equivalence between the quantum evolution of spatially homogeneous oscillations of a scalar field and that of an analogous classical system with certain random initial condition. We argue that this observation can be used for numerical simulation of the Universe in the preheating epoch. We also explicitly demonstrate that the phenomenon of parametric resonance that leads to preheating is simultaneously an effective mechanism for generating quantum decoherence of the Universe.

UW-PT-96-01

1. Calculation of the reheating temperature is one the most important issue in inflationary cosmology. The temperature achieved soon after the inflation epoch is the maximum temperature in the whole history of the Universe and must be sufficiently large for the generation of baryon number to be effective. According to the inflationary picture, the Universe is reheated by the process of transferring energy out of spatially homogeneous oscillations of the scalar inflation field. The old theory of the reheating [1] describes this energy transfer as occurring through the decay of the inflation quanta and predicts a relatively low speed for this process in theories with small coupling constants. However, a recent revision [2] shows that in many cases there exists a more rapid channel of energy transfer, which is closely related to the existence of parametric resonance in the spectra of the fields interacting with the inflation and of the inflation itself. These parametric resonance modes, typically forming continuous energetic bands, grow exponentially on the background of the inflation field oscillations, and at some moment begin to take a large amount of energy from these oscillations. It has been argued in ref.[2] that due to the exponential character of the growth, the decay of the inflation field oscillations is a rapid process of "explosion" rather than a slow damping. The amplitude of these oscillations drops to a small value after some time interval of the same order as of magnitude of the period of oscillations. This new mechanism, named in ref.[2] "preheating", may change considerably the prediction of the reheating temperature. It has been argued that the phenomenon of parametric resonance may be important in other aspects as well [3, 4].

The complete theoretical description of preheating is still lacking right now, due to the complexity of interaction between the modes that appear via parametric resonance and the background, as well as between the modes themselves. However, some important steps have been made in this direction (see, for example [5, 6]). In one of the approaches [6] the problem is treated in the Hartree-Fock approximation, where one takes into account the backreaction of the parametric resonance modes to the background but neglects the scattering between these modes. The result is quite surprising: while it confirms that parametric resonance is the main mechanism of the damping of the inflation field in the first time period, in the long run the amplitude of the oscillations typically remains constant (in some cases it is not much smaller than the initial amplitude before the explosion), or at least decays very slowly. This shows that it takes much longer time, of many order of magnitudes larger than the period of oscillations, to make the amplitude goes to 0. At late times, the created particles are mostly of very small energy, which means that the thermalization pro-

process may also take a longer time interval than has been expected. The calculations in ref.[6], however, rely heavily on the Hartree-Fock approximation, so there remains the question whether these results reflect the real situation.

In this paper we do not attempt to build a complete theory of preheating. However, we will point out a possible way to perform reliable calculations in the nonlinear regime after inflation. Namely, we show that the behavior of the quantum system under consideration, during the preheating epoch, is equivalent to the evolution of the classical field, when one randomizes over a particular set of initial conditions. This result is established by comparing the perturbative series of the two theories. This fact makes possible numerical simulations of the Universe after inflation, since the problem is now completely classical. As a by-product, we demonstrate explicitly the development of decoherence of the Universe. We show that the phenomenon of parametric resonance provides an effective mechanism for the latter.

2. For simplicity we will work in the model of one scalar field only. In other words, we neglect the interaction of the inflaton with other particles and take into account its self-interaction only. The Lagrangian of the model is taken in the standard form,

$$L = \frac{1}{2} (\partial_\mu \phi)^2 - \frac{m^2}{2} \phi^2 - \frac{\lambda}{4!} \phi^4$$

We will also neglect the expansion of the Universe and work in the ordinary Minkowski space-time. At the moment when inflation completes, the inflaton field has a nonzero expectation value $\phi = \phi_0$ which is a constant over the whole space. Soon after that the field begins oscillations around $\phi = 0$. For convenience the following picture is used in further discussions: at $t < 0$ there is an extra force term J in the Lagrangian so that the expectation value of ϕ is a nonzero constant ϕ_0 , but at $t = 0$ this source is suddenly turned off and the field starts oscillate. We will be interested in the time dependence of the mean value of ϕ , which will be denoted as $\langle \phi \rangle(t)$.

The linearized classical equation for the modes of momentum k of the field, $(t; k)$,

$$\partial_t^2 + k^2 + \frac{\lambda}{2} \phi_0^2(t) \quad (t; k) = 0 \quad (1)$$

has the same form as that of the oscillator whose frequency is a periodic function of time, $k^2 = k^2 + \frac{\lambda}{2} \phi_0^2(t)$. It is well known that at some values of k this system exhibits parametric resonance: there does not exist any solution to eq.(1) which remains finite on the whole time axis [7]. A typical solution to eq.(1) grows exponentially in the limits $t \rightarrow +1$ and/or $t \rightarrow -1$. This phenomenon occurs when k lies in

certain energetic bands ("resonance bands"). We will consider the situation of broad resonance, which correspond to large values of $\omega_0, \omega_0 \approx 1 = \frac{p}{m}$ or larger.

In the quantum case, the existence of parametric resonance leads to the amplification of the quantum fluctuations of the modes with ω_k inside the resonance bands. When the amplitude of these fluctuations are still small, one can make use of the standard Bogoliubov transformations to find the quantum state of the system [5]. However, the interesting regime is that of late times where the non-linearity becomes essential, and one needs another approach to attack the problem.

The general method to find real-time evolution of quantum fields is the Schwinger-Keldysh closed-time-path formalism [8, 9, 10]. At diagrammatic level, the formalism gives rise to the same set of Feynman rules as that for calculating the S-matrix, except that every internal integral in Feynman diagrams is now performed along a contour that goes from $t = -1$ to $t = +1$ and then goes back to $t = -1$ (Fig.1), and instead of one Feynman propagators $G(x; y)$ there exists four ones depending on whether x_0 and y_0 lie on the upper or the lower parts of the contours,

$$G_{++}(x; y) = \langle 0 | T(x)(y) | 0 \rangle; \quad G_{+-}(x; y) = \langle 0 | (y)(x) | 0 \rangle;$$

$$G_{-+}(x; y) = \langle 0 | (x)(y) | 0 \rangle; \quad G_{--}(x; y) = \langle 0 | T(x)(y) | 0 \rangle;$$

It is easy to see that these propagators arise from the propagators on the contour C , $G_C(x; y) = \langle 0 | T_C(x)(y) | 0 \rangle$, where T_C is the notation for time-ordering along C . Note also that the four propagators are equal at $x = y$.

To derive the Feynman rules, we will decompose the quantum field into a classical part $\phi_0(t)$ and quantum fluctuation $\tilde{\phi}$,

$$\phi(t) = \phi_0(t) + \tilde{\phi}(t)$$

where $\phi_0(t) = \phi_0$ at $t < 0$ and at $t > 0$ satisfies the field equation

$$\partial^2 \phi_0 + m_0^2 \phi_0 + \frac{\lambda}{3} \phi_0^3 = 0$$

The Lagrangian for $\tilde{\phi}$ is then

$$L(\tilde{\phi}) = \frac{1}{2} (\partial_\mu \tilde{\phi})^2 - \frac{m^2}{2} \tilde{\phi}^2 - \frac{\lambda}{4} \phi_0^2 \tilde{\phi}^2 - \frac{\lambda}{3!} \phi_0 \tilde{\phi}^3 - \frac{\lambda}{4!} \tilde{\phi}^4$$

and corresponds to the Feynman rules shown in Fig.2.

Before turning to the calculation of diagrams, let us consider in more details the propagators on the background $\phi_0(t)$. Consider, for instance, $G_{++}(x; y)$. It is

convenient to use the mixed representation (coordinate in time and momentum in space) where this propagators can be written into the form ,

$$G_{++}(\mathbf{x};\mathbf{y}) = \int \frac{d\mathbf{k}}{(2\pi)^3} e^{i\mathbf{k}(\mathbf{x}-\mathbf{y})} G_{++}(\mathbf{x}_0;\mathbf{y}_0;\mathbf{k})$$

where

$$iG_{++}(\mathbf{x}_0;\mathbf{y}_0;\mathbf{k}) = (\mathbf{x}_0 - \mathbf{y}_0) f_1^k(\mathbf{x}_0) f_2^k(\mathbf{y}_0) + (\mathbf{y}_0 - \mathbf{x}_0) f_2^k(\mathbf{x}_0) f_1^k(\mathbf{y}_0) \quad (2)$$

We have introduced the mode functions $f_{1,2}^k$ which are the two linearly independent solutions to the equation

$$\partial_t^2 + \omega_k^2 + \frac{1}{2} \omega_0^2(t) f_{1,2}^k(t) = 0 \quad (3)$$

with the following boundary conditions at $t < 0$,

$$f_1^k(t) = e^{i\omega_k t}; \quad f_2^k(t) = e^{i\omega_k t}$$

where $\omega_k = \sqrt{k^2 + m^2 + \frac{\omega_0^2}{2}}$. The mode functions are normalized so that $f_1^0(t) f_2^0(t) = 1$. If $\omega_0(t)$ is 0, f_1^k and f_2^k would be equal to $e^{i\omega_k t} \sqrt{\frac{1}{2\omega_k}}$ and $e^{i\omega_k t} \sqrt{\frac{1}{2\omega_k}}$, respectively. It is easy to see that $f_2^k(t) = (f_1^k(t))^*$.

The formulas for other propagators are similar,

$$iG_{+-}(\mathbf{x}_0;\mathbf{y}_0;\mathbf{k}) = f_2^k(\mathbf{x}_0) f_1^k(\mathbf{y}_0)$$

$$iG_{-+}(\mathbf{x}_0;\mathbf{y}_0;\mathbf{k}) = f_1^k(\mathbf{x}_0) f_2^k(\mathbf{y}_0)$$

$$iG_{--}(\mathbf{x}_0;\mathbf{y}_0;\mathbf{k}) = (\mathbf{x}_0 - \mathbf{y}_0) f_2^k(\mathbf{x}_0) f_1^k(\mathbf{y}_0) + (\mathbf{y}_0 - \mathbf{x}_0) f_1^k(\mathbf{x}_0) f_2^k(\mathbf{y}_0) \quad (4)$$

Consider now a value of k where there is parametric resonance in eq.(3). When parametric resonance is present, eq.(3) possesses two real solutions $f_+^k(t)$ and $f_-^k(t)$ which satisfy the following conditions at $t > 0$ [7],

$$f_+^k(t+T) = e^{\gamma_k T} f_+^k(t)$$

$$f_-^k(t+T) = e^{-\gamma_k T} f_-^k(t)$$

where γ_k is some real, positive constant depending on ω_k . In particular, f_+ grows as $t!^{+1}$ while the behavior of f_- is opposite. The previously defined mode functions f_1 and f_2 are linear combinations of f_+ and f_- . Not interested in the particular form of the coefficients, we write,

$$f_1^k(t) = \alpha_k f_+^k(t) + \beta_k f_-^k(t); \quad f_2^k(t) = \gamma_k f_+^k(t) + \delta_k f_-^k(t); \quad (5)$$

where we have made use of the fact that f_1 and f_2 are complex conjugate and f_+ and f_- are real. Since as f_+ is growing with t while f_- is falling, at large t the part $f_+(t)$ dominates over $f_-(t)$. If in eq.(5) one neglects f_- and leaves only f_+ , there is no difference between f_1 and f_2 , except for an overall factor. If one also neglects modes outside resonance bands, which is natural since these modes are not enhanced, and substituting eq.(5) to eqs.(2), (4) one finds that the four propagators are equal to each other to the leading order,

$$\begin{aligned} iG_{++}(x;y) &= iG_{+-}(x;y) = iG_{-+}(x;y) = iG_{--}(x;y) = \\ &= iG^0(x;y) = \frac{1}{(2\pi)^3} \int_k f_+^k(x_0) f_+^k(y_0) \end{aligned} \quad (6)$$

Now let us consider the one-loop contribution to χ_1 . The only diagram that contributes to χ_1 is the tadpole one shown in Fig.3a. This diagram is equal to

$$\chi_1(x) = \frac{1}{2} \int_{-c}^Z dy_0 \int_c^Z dy G_C(x;y) G^0(y_0) G(y;y) = \frac{1}{2} \int_c^Z dy G_R(x;y) G^0(y_0) G(y;y) \quad (7)$$

where we have dropped the indices of $G(y;y)$ since all the four Green functions are equal at coinciding points and introduced the retarded Green function, $G_R = G_{++} - G_{+-}$. One can expect that at late x_0 the integral in eq.(7) is dominated by large values of y_0 where $G(y;y)$ can be replaced by the leading term, eq.(6). So one finds,

$$\chi_1(x_0) = \frac{1}{2} \int_c^Z dy_0 G_R(x_0; y_0; 0) G^0(y_0) \frac{1}{(2\pi)^3} \int_k f_+^k(y_0) f_+^k(y_0) \quad (8)$$

Eq.(8) can be represented graphically as in Fig.3b, where each external line ending with a bullet is associated with the factor $\int_k f_+^k(y_0)$ if k is a resonance mode and 0 in the opposite case. Note that f_+^k grows exponentially with t , so χ_1 is also growing. At t when χ_1 becomes comparable to χ_0 one can expect that all terms of the perturbative series are of the same order, and the perturbation theory breaks down. We will try to extract the main contribution from each order of the perturbation theory in this regime. We will not be interested at latter times when $\chi_1 \gg \chi_0$.

Let us move to two-loop diagrams. Consider, for example, the one depicted in Fig.4a,

$$\chi_2(x_0) = \frac{1}{2} \int_{-c}^Z dy_0 \int_c^Z dz_0 \frac{1}{(2\pi)^3} G_C(x_0; y_0; 0) G^0(y_0) G_C(y_0; z_0; k) G_C(y_0; z_0; k) G^0(z_0) \chi_1(z_0) \quad (9)$$

If one is interested large values of x_0 , it can be expected that the important region of integration in r.h.s. of eq.(9) is that of large y_0 and z_0 . So, one may suspect that the integral can be calculated by replacing $G_C(x_0; y_0; k)$ by its leading order contribution, eq.(6). One obtains after that

$$_2(x_0) = \frac{i^2}{2} \int_C^Z dy_0 dz_0 \frac{dk}{(2\pi)^3} G_C(x_0; y_0; 0) f_+^k(y_0) (f_+^k(y_0))^2 (f_+^k(z_0))^2 f_+^k(z_0) \quad (9)$$

However, it is easy to see that the integration over z_0 gives zero, since it goes along the contour C and the integrand, $(f_+^k(z_0))^2 f_+^k(z_0)$, is the same on the upper and lower parts of the contour. So, one should turn to the next{to{leading order. Denoting the next correction to eq.(6) as $G_C^1(x; y) = G_C(x; y) - G^0(x; y)$, one writes,

$$\begin{aligned} _2(x_0) &= \frac{i^2}{2} \int_C^Z dy_0 dz_0 \frac{dk}{(2\pi)^3} G_C(x_0; y_0; 0) f_+^k(y_0) G_C^1(y_0; z_0; k) f_+^k(y_0) f_+^k(y_0) f_+^k(z_0) \quad (10) \\ &= \frac{i^2}{2} \int_C^Z dy_0 dz_0 \frac{dk}{(2\pi)^3} G_C(x_0; y_0; 0) f_+^k(y_0) G_C(y_0; z_0; k) f_+^k(y_0) f_+^k(y_0) f_+^k(z_0) \end{aligned}$$

where in the last equation we have replaced G_C^1 by G_C , making use of the fact that the leading term vanishes. Eq.(10) can be rewritten in a simpler form using the retarded propagator $G_R = G_{++} - G_+$,

$$_2(x_0) = \frac{i^2}{2} \int_{-1}^Z dy_0 dz_0 \frac{dk}{(2\pi)^3} G_R(x_0; y_0; 0) f_+^k(y_0) G_R(y_0; z_0; k) f_+^k(y_0) f_+^k(y_0) f_+^k(z_0) \quad (11)$$

where the integrations over dy_0 and dz_0 are performed from -1 to $+1$. Eq.(10) can be represented graphically as in Fig.4b. As in the case of the one{loop graph, the calculation of the loop diagram, thus, is reduced to evaluation of a tree connected graph.

This technique can be generalized to deal with other diagrams and higher orders of perturbation theory. Summarily, the technique is the following. To calculate a given Feynman diagram with l loops, one cuts l internal propagators, so that the obtained diagram is tree, and connected. If there are m many ways to perform this cutting, one should take a sum over all possibilities. Each propagator that has been cut is associated with two factors of f_+^k attached to the two vertices that the former propagator had been connecting. The propagators that have not been cut are associated with the retarded propagator G_R . The obtained diagrams are computed by the standard way, where the integral are performed along the usual time axis. We note that this

reduction of loop graphs to tree ones is very similar to that found in another setting [11]. We emphasize that our method is applicable in the regime when all terms of the perturbation series are of the same order. At latter times when $t \rightarrow 0$ our approach does not work, since the pieces that have been neglected may become important.

3. The fact that the diagrams obtained after the cutting procedure are tree points to the possibility of classical description of the problem. To end the latter, let us consider the Cauchy initial problem with the classical field equation

$$(\partial^2 + m^2) \phi + \phi^3 = 0 \quad (11)$$

with the following initial condition at the asymptotics $t \rightarrow 1$,

$$\phi(t; x) = \phi_0(t) + \int \frac{dk}{(2\pi)^3} c_k f_+^k(t) e^{ikx} \quad (12)$$

where c_k are some arbitrary set of complex numbers. For ϕ to be real, we require that $c_k = c_k^*$. Since at $t \rightarrow 1$ $f_+^k(t)$ is small and satisfies eq.(3), eq.(12) is the solution to the field equation up to the first order of f_+ . The corrections to eq.(12), which start at the second order of f_+ , can be calculated iteratively from the field equation and the result can be represented in the form of tree Feynman diagrams. For example, the second order contribution is represented by the first diagram in Fig.5 together some third and fourth order graphs. In these graphs each external leg ending on a bullet is associated with the factor $c_k f_+^k$, and each internal line corresponds to the retarded propagator.

Despite the fact that these diagrams are similar to that obtained by the cutting procedure described above, there are two main differences between the two cases. First, the diagrams obtained by cutting loop graphs always contains an even number of external bullet legs. Second, the external bullet legs in the first case can be grouped into pairs so that the momenta running along legs of the same pair are of opposite signs, while in the graphs coming from eq.(12) the only requirement is that the sum of the momenta of the bullet legs is 0. Nevertheless, it is easy to show that there is a simple relation between the two cases. Namely, if one denotes as $\phi(t; x; c_k)$ the solution to the field equation with the boundary condition (12), then the quantum average of ϕ in our problem is given by an integral over c_k with a Gaussian measure,

$$\langle \phi(t) \rangle = \int D c_k \exp \left[- \int \frac{dk}{(2\pi)^3} \frac{j_k j_{-k}}{2j_k^2} \right] \phi(t; x; c_k) \quad (13)$$

(the integral in the r.h.s. of eq.(13) does not depend on x). To see this, one notices that the integration over $D c_k$ leaves only diagrams with even number of bullet legs

which can be grouped in paired of opposite momenta. The integration also adds a factor of j_k^2 to each pair with momentum $(k; -k)$. So, the graphical representation of the r.h.s. of eq.(13) is the same as those obtained by cutting the loop graphs.

In eq.(13), c_k are supposed to be real, Gaussian distributed around 0 with the standard deviation j_k and the c_k with different k are not correlated. Eq.(13) is not the only possible, one could write, for example

$$\phi(t) = \sum_k D_k \left[\phi(x; j_k) \exp(i k x) \right] \quad (14)$$

where c_k now are complex numbers with fixed absolute value equal to j_k but with random phase. One can write more relations of this type.

Eqs.(13,14) give rise to the possibility of numerical simulation of the processes occurring in the Universe after inflation. To do this it is sufficient to take an initial field configuration in the form of a homogeneous oscillations plus appropriate random perturbations, and evolve this configuration in time according to the field equation. The mean value of ϕ in this classical system is the same as that of the quantum one. It is trivial to derive the same result in theories with more than one scalar fields.

Eqs.(13,14) are the manifestation of the fact that when the amplitude of quantum fluctuations is large (roughly speaking, when the occupation numbers are large), the system behaves like a classical one. Our derivation gives this statement a precise meaning.

It is also interesting to mention the relation between eq.(13,14) and the fundamental phenomenon of decoherence of the Universe. In a situation when, as in our case, a closed system starts its evolution from a quantum pure state at $t = 0$ it will remain in a pure state at any time moment. The system that we are considering can be described, in the pure state language, by the operators obtained by Bogoliubov transformation [5]. However, when the resonance modes become large the modes strongly interact between themselves and the pure state description becomes very complicated. In rescue, another description comes into effect: the system can be considered as a mixed state, i.e. that of an ensemble, of states (semiclassical in our case) characterized by the solution to the field equation with initial condition (12) with c_k playing the role of the indices numbering the quantum states in the ensemble. Explicitly, the system is described by the following density matrix,

$$\hat{\rho} = \sum_{c_k} j_k \left| \phi(x; c_k) \right\rangle \langle c_k | \phi(x; c_k) \rangle$$

where $j_k \left| \phi(x; c_k) \right\rangle$ is the notation for a (pure) semiclassical quantum state associated

with the classical field configuration $\{\phi; \mathbf{x}; c_k\}$ (the choice of $j \{\phi; \mathbf{x}; c_k\}$ is not unique). Eq.(13,14) ensures that the average of ϕ in this mixed state is equal to its true quantum average in the pure state with proper choice of $\{c_k\}$. It can be shown that the same is valid for other Green functions as well. So, for calculating physical quantities one can consider the system as being in a mixed state, though in fact its true state is a pure one. Note that the time period when c_k are large, $c_k \gg 1$, but still sufficiently small so that the modes are linear, is the matching region where both pure and mixed state descriptions can be used.

4. So, we have shown that the problem of evolution of the homogeneous oscillating scalar field that has a direct connection with preheating in inflationary cosmology is equivalent to the classical evolution of the scalar field with some random initial conditions. We also show that the parametric resonance phenomenon provides an effective mechanism for the generation of decoherence of the Universe. We have seen a nice feature of this mechanism that the transition from the pure state to mixed state description can be traced explicitly.

The result of this paper may be useful for numerical modeling of the preheating process and hopefully will lead to the better understanding of the latter. Preliminary results seem to agree qualitatively with that of the Hartree-Fock approximation: the fall of the amplitude of oscillations is saturated at some finite level. Moreover, after this saturation the modes with small k seem to play an important role in the evolution. The work is still continuing, results will be published elsewhere.

The author thanks P. A. Mold, V. Rubakov, P. Tinyakov and L. Ya. for valuable discussions.

References

- [1] A.D. Dolgov and A.D. Linde, Phys. Lett. 116B, 329 (1982); L.F. Abbot, E. Farhi, and M. Wise, Phys. Lett. 117B, 29 (1982).
- [2] L. Kofman, A.D. Linde, and A.A. Starobinsky, Phys. Rev. Lett. 73, 3195 (1994).
- [3] L. Kofman, A. Linde, and A. Starobinsky, Nonthermal Phase Transitions After Inflation, preprint SU-ITP-95-21, UH-IA-95/51, hep-th/9510119.
- [4] I.I. Tkachev, Phase Transitions at Preheating, preprint OSU-TA-21/95, hep-th/9510146.
- [5] Y. Shtanov, J. Traschen, and R. Brandenberger, Phys. Rev. D 51, 5438 (1995).
- [6] D. Boyanovsky, H.J. de Vega, R. Holman, D.-S. Lee, and A. Singh, Phys. Rev. D 51, 4419 (1995).
- [7] L.D. Landau and E.M. Lifshits, Mechanics, Pergamon Press, 1976.
- [8] E.M. Lifshits and L.P. Pitaevskii, Physical Kinetics, Pergamon Press, 1981.
- [9] E. Calzetta and B.L. Hu, Phys. Rev. D 35, 495 (1988); Phys. Rev. D 37, 2838 (1988).
- [10] J.P. Paz, Phys. Rev. D 41, 1054 (1990); Phys. Rev. D 42, 529 (1990).
- [11] M.V. Libanov, V.A. Rubakov, D.T. Son, and S.V. Troitsky, Phys. Rev. D 50, 7553 (1994).

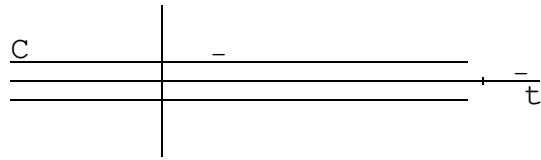


Figure 1: Integration contour in Schwinger-Keldysh formalism.

$$T_T \text{ --- } i \int_0^{\infty} dt \, e^{i t (\mathcal{Q}^2 + m^2 + \frac{1}{2} \frac{\partial^2}{\partial t^2})^{-1}}$$

Figure 2: Feynman rules for calculating $\Gamma(t)$.

$$\text{---} \quad \text{---} = \text{---} \begin{matrix} T \\ T \\ T \\ t \end{matrix}$$

a a'

Figure 3: The one-loop graph (a) and the representation (b) of its leading contribution.

$$\text{---} \quad \text{---} = \text{---} \begin{matrix} t & t & t \\ | & | & \\ T & T & T \\ t & t & t \end{matrix}$$

b b'

Figure 4: A two-loop graph (a) and its reduction to a tree graph (b).

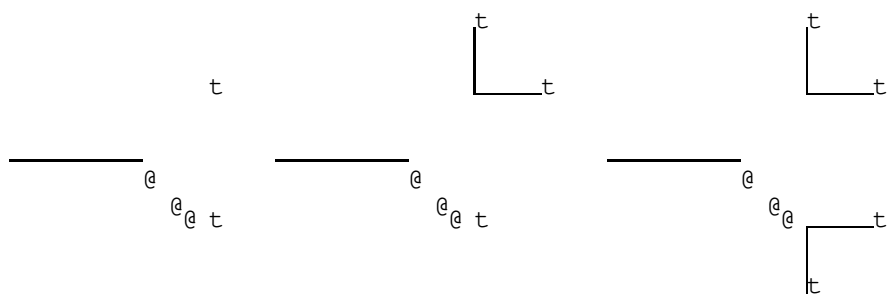


Figure 5: Some tree diagrams arising from the classical problem.